

Highly tunable and temperature insensitive multilayer barium strontium titanate films

S. Zhong and S. P. Alpay^{a)}

Materials Science and Engineering Program, University of Connecticut, Storrs, Connecticut 06269

M. W. Cole, E. Ngo, S. Hirsch, and J. D. Demaree

Weapons & Materials Research Directorate, Active Materials Research Group U.S. Army Research Laboratory, Aberdeen Proving Ground, Maryland 21005

(Received 5 January 2007; accepted 26 January 2007; published online 27 February 2007)

Multilayered $\text{Ba}_{1-x}\text{Sr}_x\text{TiO}_3$ (BST) films were deposited on Pt coated Si substrates via metalorganic solution deposition. The multilayer heterostructures consisted of three distinct layers of ~ 220 nm nominal thickness with compositions corresponding to BST 63/37, BST 78/22, and BST 88/12. At room temperature, the heterostructure has a small-signal dielectric permittivity of 360 with a dissipation factor of 0.012 and a dielectric tunability of 65% at 444 kV/cm. These properties exhibited minimal dispersion as a function of temperature ranging from 90 to -10 °C. These results are explained via a thermodynamic model that incorporates electrical, mechanical, and electromechanical interactions between BST layers. © 2007 American Institute of Physics.

[DOI: 10.1063/1.2710005]

Due to their highly nonlinear dielectric response to an applied electric field, ferroelectric (FE) materials have attracted significant interest as active elements of tunable microwave (MW) devices for wireless telecommunications.^{1,2} $\text{Ba}_{1-x}\text{Sr}_x\text{TiO}_3$ (BST) is one of the leading candidates for such applications since the dielectric response and its tunability are very high in the vicinity of the paraelectric (PE) to FE phase transformation temperature T_C which can be controlled via the composition [e.g., the bulk T_C of BST 60/40 ($\text{Ba}_{0.60}\text{Sr}_{0.40}\text{TiO}_3$) is just below room temperature (5 °C)].³⁻⁷ The major challenge in designing materials systems for tunable devices is the simultaneous requirement of high tunability ($>40\%$) over a large temperature interval (-20 to $+85$ °C) coupled with low dielectric losses (between 3.0 and 4.0 dB in operational bandwidths ranging from several hundred megahertz up to 30 GHz or more).

While the dielectric losses in BST films can be greatly reduced by additions of metallic dopants,⁸ tunability of monolithic BST films is strongly dependent on the temperature. Multilayer and graded ferroelectrics display little temperature dependence in the dielectric behavior due the variations in T_C that results in a “diffuse” phase transformation^{9,10} and the tunability can be maximized by optimizing the internal electric fields that arise between layers due to the polarization mismatch.¹¹ Theoretical results indicate that the range where the dielectric tunability is relatively constant can be adjusted via the composition of the BST layers and their relative volume fractions.¹¹ In this letter, we present an experimental and theoretical study on BST multilayer films with systematic variations in the composition that display both high tunability over a wide range of temperature and low loss. The theoretical approach is based on a nonlinear thermodynamic model that incorporates electrical, mechanical, and electromechanical interactions between BST layers. The excellent agreement between experimental findings and the theoretical calculations suggests that the theoretical for-

malism can be used as a predictive tool to design tunable devices for telecommunications.

Experimentally, multilayered BST films were fabricated on Pt coated high resistivity Si substrates (PtSi) via the industry standard metal-organic solution deposition (MOSD) technique using carboxylate-alkoxide precursors. A detailed description of the MOSD precursor solution preparation and film deposition technique has been reported elsewhere.^{12,13} The multilayer heterostructure of ~ 220 nm nominal thickness was synthesized from three precursors with compositions corresponding to BST 60/40, BST 75/25, and BST 90/10 which were sequentially deposited onto the PtSi substrates. A schematic of the multilayer heterostructure is shown in Fig. 1(a). After each individual spin-on film coat-

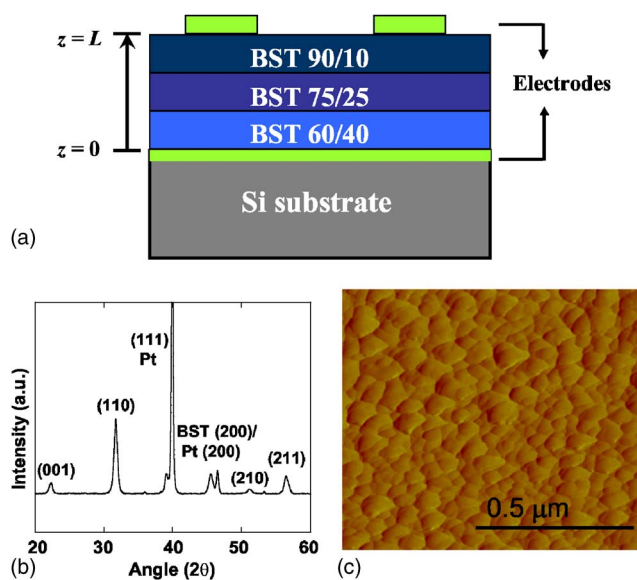


FIG. 1. (Color online) (a) Schematic configuration of BST multilayer heterostructure with total thickness of 220 nm sandwiched between metallic electrodes. (b) X-ray diffraction pattern of the BST multilayer. (c) AFM micrograph showing the plan-view surface morphology of the BST multilayer with roughness of 3.479 nm.

^{a)} Author to whom correspondence should be addressed; electronic mail: p.alpay@ims.uconn.edu

ing, the sample was pyrolyzed at 350 °C for 10 min in order to remove the organic addenda and then annealed at 750 °C for 60 min in flowing oxygen. This ensured that each distinct layer composition was fully crystallized prior to the deposition of the next compositional layer.

X-ray diffraction (XRD) analysis using a Rigaku diffractometer with Cu $K\alpha$ radiation at 40 kV showed that the multilayered BST films exhibited a random polycrystalline perovskite structure and there was no evidence of secondary phase formation since no peaks other than the (100), (110), (111), (200), (210), and (211) BST were observed [Fig. 1(b)]. The surface morphology of the heterostructures was assessed via atomic force microscopy (AFM) over a $1 \times 1 \mu\text{m}^2$ scan area [Fig. 1(c)] using a Digital Instruments Dimension 3000 tapping mode AFM. Films exhibited a dense microstructure with no cracks, pinholes, or other surface defects. The surface roughness as quantified by AFM was found to be ~ 3.5 nm. Rutherford backscattering spectroscopy with 2 MeV He⁺ ion beam from a NEC 5SDH-2 tandem positive ion accelerator was employed to analyze film composition and film thickness. All spectra were fitted and interpreted using the program RUMP.¹⁴ The heterostructure was found to consist of three distinct layers with compositions BST 63/37, BST 78/22, and BST 88/12. A detailed study of the microstructure and compositional analysis will be presented elsewhere.

Electrical measurements were carried out in the metal-insulator-metal capacitor configuration, with Pt as both the top and bottom electrodes. The film capacitance C and dissipation factor $\tan \delta$ were measured with an HP 4194A impedance/gain analyzer at 100 kHz. The tunability, $\eta = \Delta C/C_0$, where ΔC is the change in capacitance relative to zero-bias capacitance C_0 , was measured as a function of applied bias from 0 to 444 kV/cm. The measurements were performed as cycle sweeps (negative voltage to positive voltage back to negative voltage) to check for any possible hysteretic behavior. The temperature dependence of the dielectric properties were determined using an in-house temperature measurement apparatus consisting of a temperature control box equipped with a Peltier thermoelectric module heating stage in an inert ambience. The dielectric properties (dielectric loss and capacitance-voltage measurements) were assessed from 90 to -10 °C in incremental temperature steps of 10 °C. The maximum rate of cooling/heating the samples was less than 1 °C/min with a settling time of 30 min at each designated measurement temperature.

The small-signal dielectric permittivity and $\tan \delta$ are plotted in Fig. 2(a) as a function of temperature. At room temperature (RT=25 °C), the multilayer film exhibited a higher permittivity ($\chi=360$) and lower dissipation factor ($\tan \delta=0.012$). Figure 2(a) demonstrates that both χ and $\tan \delta$ of the heterostructure exhibited minimal dispersion as a function of temperature ranging from 90 to -10 °C. The tunability as a function of temperature and applied electric field is shown in Fig. 2(b). As expected, the tunability increases with increasing electric field at all temperatures. At RT, the tunability is 65.5% at 444 kV/cm. Furthermore, Fig. 2(b) clearly shows that over the temperature range of -10 –90 °C, the tunability is not significantly degraded.

To understand these results, a thermodynamic model was constructed. Consider a multilayer consisting of three BST layers with the same thickness grown on Si substrate between electrodes, as shown in Fig. 1(a). An inhomogeneous

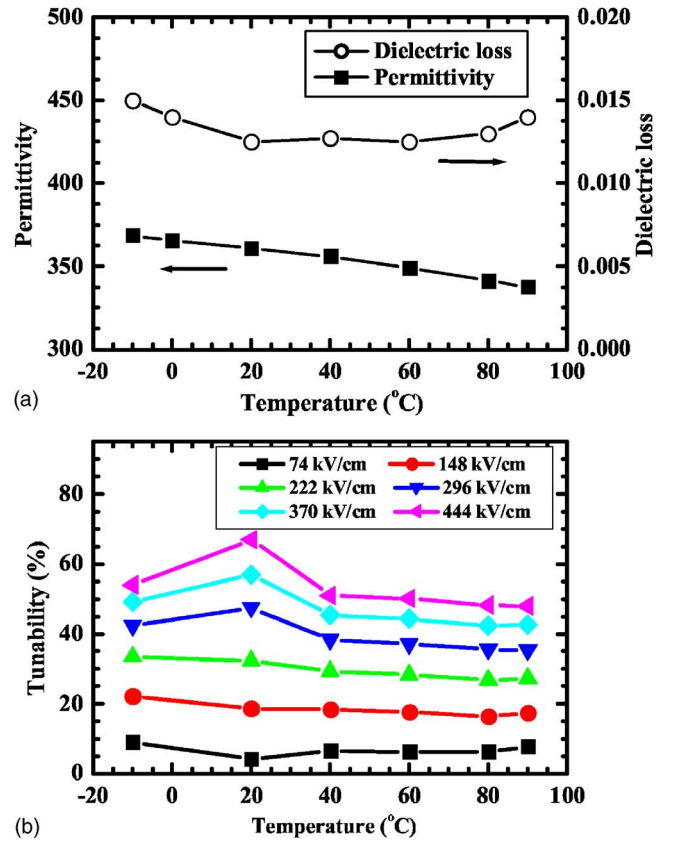


FIG. 2. (Color online) (a) Dielectric permittivity and dielectric loss of BST multilayer films as a function of operation temperature. (b) Temperature dependence of tunability at a function of external electric field.

internal in-plane strain [$u_T(z)$] arises from thermal stresses resulting from cooling down from the annealing temperature. This strain can be determined from the difference between the coefficients of thermal expansion (CTE) of the BST layers and the substrate, such that $u_T(z) = [\alpha_F(z) - \alpha_S] \Delta T$, where $\alpha_F(z)$ and α_S are the CTEs of the layers and the substrate, respectively. ΔT is the difference between annealing temperature (750 °C) and room temperature (RT=25 °C).

The free energy density of a multilayer heterostructure, as shown in Fig. 1, can be expressed through

$$F_\Sigma = F_0 + \int_0^L \left[\frac{1}{2} \bar{a}_i P_i^2 + \frac{1}{4} \bar{b}_i P_i^4 + \frac{1}{6} c_i P_i^6 + A_i \left(\frac{dP}{dz} \right)^2 - \frac{1}{2} E_{di} P_i - E P_i \right] dz + F_S, \quad (1)$$

where F_0 is the energy in the PE state and $P_i(z)$ is polarization in layer i . F_S is the interfacial energy due to the polarization variation across the interlayer interfaces between layers and can be neglected for layer thicknesses much larger than the correlation length of ferroelectricity (~ 1 –10 nm).

In Eq. (1), \bar{a}_i and \bar{b}_i are the renormalized dielectric stiffness coefficients given by¹⁵

$$\bar{a}_i = a_i - u_T \frac{4Q_{12,i}}{S_{11,i} + S_{12,i}}, \quad \bar{b}_i = b_i + \frac{2Q_{12,i}^2}{S_{11,i} + S_{12,i}}, \quad (2)$$

where a_i is the bulk dielectric stiffness coefficient, which follows the Curie-Weiss law, $a_i = (T - T_{C,i}) / \epsilon_0 C_i$, where $T_{C,i}$ and C_i are the Curie-Weiss temperature and constant of layer i and ϵ_0 is the permittivity of free space. b_i and c_i in Eqs. (1)

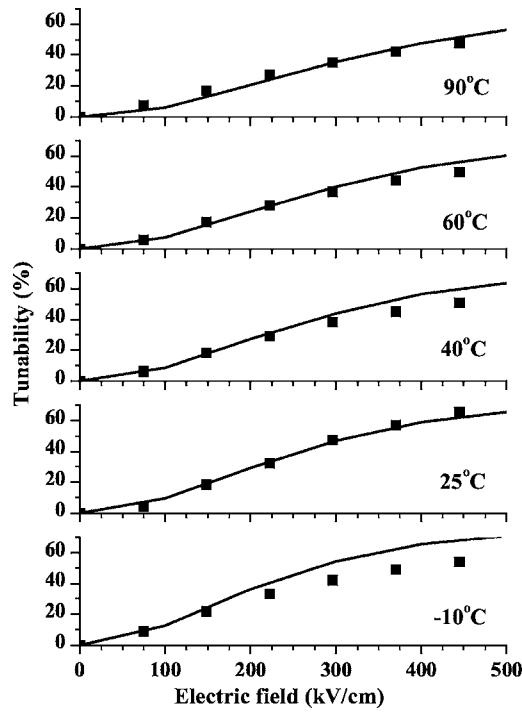


FIG. 3. Tunability of the BST multilayer as a function of external electric field at different temperatures (solid line: calculation results from theory and solid squares: experimental measurements).

and (2) are higher order stiffness coefficients of layer i . In Eq. (1), $Q_{12,i}$ are the electrostrictive coefficients, $S_{11,i}$ and $S_{12,i}$ are the elastic compliances at constant polarization, and A_i are the Ginzburg coefficients of layer i . A_i can be estimated as $A_i = |a_i| \xi_i^2$, where ξ_i is the correlation length of layer i . E is the external electric field and $E_{d,i}$ is the internal “built-in” electric field due to polarization variations such that¹⁶

$$E_{d,i} = -\frac{1}{\epsilon_0}(P_i - \bar{P}), \quad (3)$$

where \bar{P} is the average polarization of the entire multilayer. The equilibrium polarization can be determined by the equation of state ($\partial F_{\Sigma} / \partial P_i = 0$) that yields an Euler-Lagrange relation with $(dP_i / dz)|_{z=0,L} = 0$ as the boundary conditions. The average dielectric permittivity follows from

$$\chi(E) = L \left(\int_0^L \{1 / [\chi(z) + 1]\} dz \right)^{-1} - 1, \quad (4)$$

where $\chi(z) = [P_i(E + \Delta E) - P_i(E)] / (\Delta E \epsilon_0)$ is the small-signal dielectric permittivity. The tunability $\eta(E)$ in the presence of an external electric field E can thus be determined from

$$\eta(E) = \frac{\chi(E=0) - \chi(E)}{\chi(E=0)} \times 100\%. \quad (5)$$

Utilizing the above formalism, we were able to calculate the electric field dependent tunability of the BST multilayer heterostructure at different temperatures as a function of the

biasing field. The dielectric stiffness coefficients, elastic and electrostrictive moduli, and the CTEs of the layers and the substrate were compiled from available literature.^{17,18} These results are shown in Fig. 3 and there is excellent agreement with the theoretical predictions and the experimental results. In the calculations at -10°C , there is a small deviation between experimental and theoretical results at fields >300 kV/cm, which may be attributed to the ambiguity in the thermodynamic parameters used in the model at low temperatures.

The experimental results together with theoretical calculations have significant technological implications. Microwave voltage-tunable phase shifter devices are expected to be operated at variable ambient temperatures with excellent reliability and accuracy. The multilayer BST heterostructure discussed in this study possesses excellent dielectric properties and both tunability and dielectric loss are stable over a broad temperature range. Combined with analytical theoretical tools to guide the design, such multilayers or graded heterostructures may be utilized in the next generation temperature insensitive tunable devices.

The work at UConn was supported by the U.S. Army Research Office through Grant No. W911NF-05-1-0528 and the National Science Foundation (NSF) under Grant No. DMR-0132918. The authors would like to thank G. Martin and C. Hubbard for the XRD data collection and W. Nothwang for assistance with the film fabrication.

- ¹A. K. Tagantsev, V. O. Sherman, K. F. Astafiev, J. Venkatesh, and N. Setter, *J. Electroceram.* **11**, 5 (2003).
- ²O. G. Vendik, E. K. Hollmann, A. B. Kozyrev, and A. M. Prudan, *J. Supercond.* **12**, 325 (1999).
- ³J. Im, O. Auciello, and S. K. Streiffer, *Thin Solid Films* **413**, 243 (2002).
- ⁴R. A. York, A. S. Nagra, P. Periaswamy, O. Auciello, S. K. Streiffer, and J. Im, *Integr. Ferroelectr.* **34**, 1617 (2001).
- ⁵Q. X. Jia, J. R. Groves, P. Arendt, Y. Fan, A. T. Findikoglu, S. R. Foltyn, H. Jiang, and F. A. Miranda, *Appl. Phys. Lett.* **74**, 1564 (1999).
- ⁶F. A. Miranda, F. W. Van Keuls, R. R. Romanofsky, C. H. Mueller, S. Alterovitz, and G. Subramanyam, *Integr. Ferroelectr.* **42**, 131 (2002).
- ⁷P. Padmini, T. R. Taylor, M. J. Lefevre, A. S. Nagra, R. A. York, and J. S. Speck, *Appl. Phys. Lett.* **75**, 3186 (1999).
- ⁸M. W. Cole, W. D. Nothwang, C. Hubbard, E. Ngo, and M. Ervin, *J. Appl. Phys.* **93**, 9218 (2003).
- ⁹K. P. Jayadevan and T. Y. Tseng, *J. Mater. Sci.: Mater. Electron.* **13**, 439 (2002).
- ¹⁰S. Zhong, S. P. Alpay, Z. G. Ban, and J. V. Mantese, *Integr. Ferroelectr.* **71**, 1 (2005).
- ¹¹S. Zhong, S. P. Alpay, and J. V. Mantese, *Appl. Phys. Lett.* **88**, 132904 (2006).
- ¹²M. W. Cole, P. C. Joshi, M. H. Ervin, M. C. Wood, and R. L. Pfeffer, *Thin Solid Films* **374**, 34 (2000).
- ¹³M. W. Cole, C. Hubbard, E. Ngo, M. Ervin, M. Wood, and R. G. Geyer, *J. Appl. Phys.* **92**, 475 (2002).
- ¹⁴L. R. Doolittle, *Nucl. Instrum. Methods Phys. Res. B* **15**, 227 (1986).
- ¹⁵N. A. Pertsev, A. G. Zembilgotov, and A. K. Tagantsev, *Phys. Rev. Lett.* **80**, 1988 (1998).
- ¹⁶R. Kretschmer and K. Binder, *Phys. Rev. B* **20**, 1065 (1979).
- ¹⁷T. Mitsui, E. Nakamura, and K. Gesi, in *Ferroelectrics and Related Substances*, Landolt-Börnstein, New Series, Group III, Vol. 16, Pt. A, edited by K.-H. Hellwege and A. M. Hellwege (Springer, Berlin, 1981).
- ¹⁸Z. G. Ban, S. P. Alpay, and J. V. Mantese, *Phys. Rev. B* **67**, 115 (2003).